

Numerical analyses for calculation of mixed-mode I/II stress intensity factors (SIFs) in edge cracked doughnut-shaped specimens subjected to diametral compression and diametral tension loads

Mohammad Reza Mohammad Aliha^{a,b} and Naghdali Choupani^{c*}

^aWelding and Joining Research Center, School of Industrial Engineering, Iran University of Science and Technology (IUST), Narmak, 16846-13114, Tehran, Iran

^bDepartment of Mechanical Engineering, Gebze Technical University, 41400 Kocaeli, Turkiye

^cDepartment of Aerospace Engineering, Faculty of Engineering, Istanbul Aydin University, 34295, Istanbul, Turkiye

ARTICLE INFO

Article history:

Received 22 December 2025

Accepted 3 March 2026

Available online

4 March 2026

Keywords:

Doughnut-Shaped Specimen (DSS)

Diametral compression point load

Diametral tensile pin loading

Mixed mode I/II

Stress intensity factors

Numerical analyses

Geometry and loading type effects

Pure mode II crack inclination angle

ABSTRACT

In this research a doughnut-shaped specimen (DSS) is utilized for analysis of mixed mode I/II (tensile/compression and in-plane shear) fracture problem. The DSS sample is a ring specimen containing two same line cracks in the inner surface of the ring that can be loaded either by diametral compression forces applied to the outer surface of ring or diametral tension force applied to the inner surface of the DSS sample. By changing the geometrical and loading parameters including crack length ratio, type of applied loading and direction of loading relative to the cracks, the state of crack tip stresses and deformations is altered. It is shown that the DSS sample under both tensile and compressive point force loading can introduce pure mode I, pure mode II and different tensile-shear, and compression-shear deformations. The variations of three fracture parameters namely modes I and II stress intensity factors (K_I and K_{II}) are determined for the DSS sample under different geometrical and loading conditions via performing several finite element analyses. It is shown that the type of applied loading (tensile or compression) has a noticeable influence on the magnitudes of crack tip parameters. The crack inclination angle corresponding to pure mode II (pure shear deformation) are also determined for both compressed and tensile DSS specimens. This angle depends on the applied loading type, crack length ratio and inner to outer ring radius ratio.

© 2026 Growing Science Ltd. All rights reserved.

1. Introduction

Structural solid engineering materials such as composites, polymers, ceramics, geo-materials, concrete, etc., are often subjected to complex states of loads and deformations with different loading rates ranging from static to dynamic and high strain impact loads. Safe operation without catastrophic failures in structures and components made of these materials needs advanced design and manufacturing of them based on the standard methods and procedures. However, the presence of some structural defects including discontinuities, cracks, imperfect bonding between layers in layered composites or 3D-printed parts, poor adhesions between the parts and joints and other stress concentrators can increase noticeably the risk of fracture and failure compared to the un-defected parts and components. In this regard, designing and analysing the structures containing sharp cracks or sharp notches (as the most important stress concentration agent), is handled and performed by the fracture-mechanics discipline.

The literature on fracture mechanics-based analysis of crack in two-dimensions is extensive and the basic concepts of this field are presented in many researches. Fracture mechanics can be divided into linear elastic fracture mechanics (LEFM) and elastic-plastic fracture mechanics (EPFM). It is important to distinguish basic modes of fracture. For a given defect, crack propagation may be accomplished in three basic modes (i) opening-mode (Mode-I), (ii) shearing-mode (Mode-II), and (iii) tearing-mode (Mode-III) as shown schematically in **Fig. 1** and their combinations that is called mixed mode I/II, mixed mode I/III and mixed mode I/II/III. The purpose of fracture-toughness testing is to determine the value of the critical stress-intensity toughness, or fracture toughness K_{Ic} , K_{IIc} , K_{IIIc} and $K_{mixed\ mode}$. Since fracture toughness index can only be determined experimentally by conducting a test on cracked sample of the desired material. Selection of appropriate specimen geometry and loading setup can help the researchers in determining a robust, reliable and correct value of the fracture toughness using

* Corresponding author.

E-mail addresses: naghdalichoupani@aydin.edu.tr (N. Choupani)

simpler methods and easier processes. Accordingly, several test methods and specimens have been proposed in the past years by many researchers to determine fracture toughness under any of the aforementioned loading modes. Depending on the material to be tested (i.e., with brittle or ductile nature of fracture and cracking behavior) different testing methodologies have been proposed. In addition, depending on the target fracture mode, different types of loads including tension, compression, bending, shear, torsion and combinations of them can be applied to the laboratory testing samples. While for ductile type materials (such as metals and soft polymers), application of direct tensile and bending type loads are more popular and convenient (Marşavina & Linul, 2020; Vantadori et al. 2023; Saenz et al, 2011; Benderly et al. 2004; Aliha et al., 2020; Haddadi et al., 2016; Ameri et al., 2021), indirect tensile and compressive type forces are preferred types of loads for brittle and quasi-brittle materials such as rocks, ceramics and concretes (Fuan et al., 2021, Shahbazian et al., 2022; Aliha et al., 2017, Mousavi et al., 2020; Gu et al., 2023, Imani et al., 2022; Marsavina et al. 2015). Furthermore, from the view point of test geometry, several configurations and shapes such as rectangular plates (Noury et al. 1988; Tutluoglu et al., 2022), beam (Fakhri et al., 2021; Wu et al., 2023), circular (Fakhri et al., 2017; Aliha et al., 2010), semi-circular (Erarslan & Aliha 2025; Pugna et al., 2020; Aliha et al., 2022; Saesaei et al. 2024; Najjar et al. 2022), hollow ring (Hanson et al., 1994; Chen et al., 2008), triangular (Aliha et al., 2013, 2016) and other miscellaneous shapes have been used in previous fracture mechanics-based investigations.

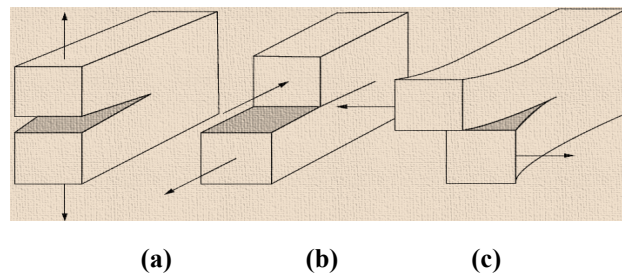


Fig. 1. Basics modes of crack extension; (a) opening-mode (Mode-I), (b) shearing-mode (Mode-II), and (c) tearing-mode (Mode-III).

For example, the utilized testing methods for two categories of engineering materials (i) layered composites and (2) geomaterials are reviewed briefly here. The double cantilever beam (DCB) test (shown in **Fig. 2a**) is the most widely used method for measuring Mode-I (opening) fracture toughness of multi-layered composite materials (Jia et al., 2021).

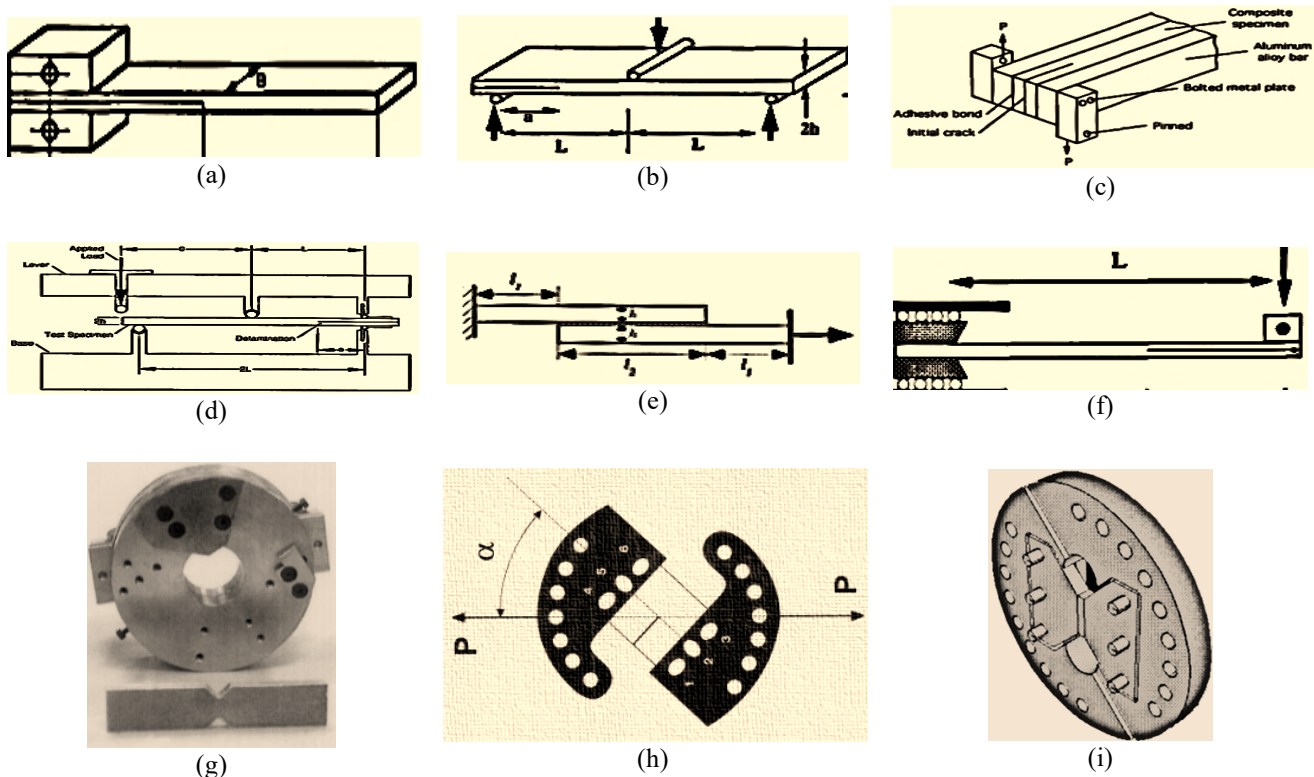


Fig. 2. Fracture toughness test configurations for testing of composite materials (a) Mode-I double cantilever beam (DCB), (b) Mode-II end-notched flexure (ENF), (c) Mode-III split cantilever rectangular beam (SCRB), (d) mixed-mode bending (MMB), (e) crack lap shear (CLS), (f) end loaded split (ELS), (g) Iosipescu, (h) Richard, and (i) modified Arcan specimens.

The end-notched flexure (ENF) shown in **Fig. 2b** has emerged as one of the most convenient Mode-II (shear) type cracking in composite materials (Gliszczynski et al., 2021; Pereira et al., 2018; Dharmawan et al., 2006). For mode-III (tearing) fracture

toughness test of composites, the split cantilever rectangular beam (SCRB) test configuration (**Fig. 2c**) is often used (Szekrényes, 2009). However, deep understanding of the fracture behavior of materials, and particularly under mixed-mode loading conditions, is needed in order to fully achieve the benefits. Various attempts have been made to characterize fracture toughness of layered composite materials under mixed-mode tensile-shear loading conditions, but mostly beam type specimens were used. The mixed-mode bending (MMB) and the crack lap shear (CLS) test specimens have been proposed by combining the schemes used for DCB and ENF tests to study the mixed-mode fracture toughness (**Fig. 2d** and **Fig. 2e**) of composite and similar materials (Choupani and Torun, 2022; Heydari et al., 2011; Choupani, 2008; Zhang et al., 2019). If the so-called end loaded split (ELS) specimen is loaded by the upper arm, mixed mode loading conditions at the crack tip are achieved (**Fig. 2f**). The ELS method has been utilized in many previous mixed mode I/II fracture studies of composite and adhesive bonding joints (Santos et al., 2017). One other type is the Iosipescu specimen (**Fig. 2g**) that has been used in different research papers (Pierron & Vautrin, 1998). Another type of specimen for studying the mixed-mode fracture toughness in composites, joints, metallic parts and etc., is the Richard specimen shown in **Fig. 2h** (Razavi and Berto, 2019). Similarly, modified Arcan specimens (**Fig. 2i**) was used for the mixed-mode fracture test (Shameli et al., 2016). The reviewed literature for the fracture toughness testing of composite materials reveals that beam or rectangular shape specimens are favorite configurations because of convenience of composite test sample preparation using these shapes.

In contrast, for a wide range and categories of construction and geo-materials including rock, soil, mortars, cement concrete and asphalt mixtures with brittle and quasi-brittle fracture nature, circular and disc shape samples seem better geometries for conducting the fracture toughness experiments. This is because of ease of sample preparation and extraction from cylindrical molds or cores obtained from such materials. In this regard, well-known and frequently used samples are: center cracked Brazilian disc (CCBD) specimen (He et al., 2022), semi-circular bend (SCB) specimen (Baradaran et al., 2024), edge notched-disc bend (ENDB) specimen (Bahmani et al., 2020, Bidadi et al., 2020, Shahbazian et al., 2022), edge-notched diametral compression disc (ENDC) specimen (Mousavi et al., 2025a,b, Bahmani et al., 2021; Bahmani and Nemati, 2021) and double notch diametral compressed disc (DNDC) specimen (Mohammadaliha et al., 2021). All the mentioned test samples in which their schematics are illustrated in Fig. 3 are capable of simulating pure mode I case and some of them can introduce mode II, mode III and mixed mode I/II, I/III and I/II/III fracture modes and can be utilized for determining K_{Ic} , K_{IIc} , K_{IIIc} and $K_{\text{mixed mode I/II}}$, $K_{\text{mixed mode I/III}}$ and $K_{\text{mixed mode I/II/III}}$.

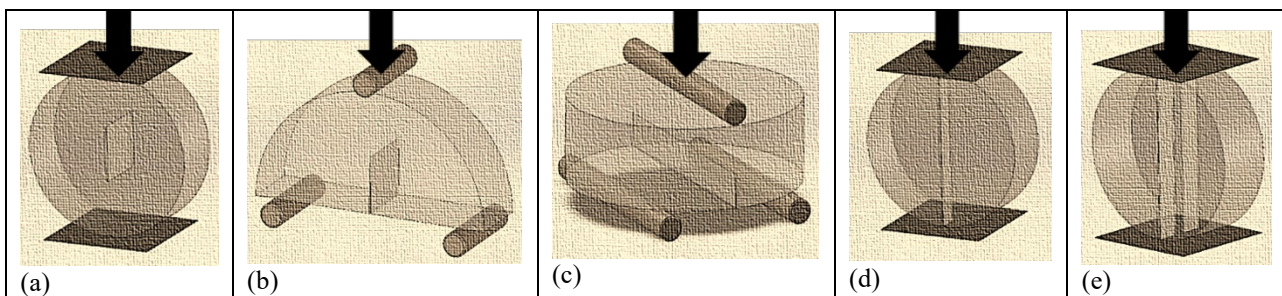


Fig. 3. Circular and disc shape samples utilized in the literature for conducting fracture tests on geomaterials (a) CCBBD, (b) SCB, (c) ENDB, (d) ENDC, (e) DNDC specimens capable of introducing pure opening mode and different combinations of opening-shearing deformations.

However, still researchers are working to propose new and novel testing methods for fracture behavior analyses of different engineering materials. Indeed, any new test method may have some benefits and advantages relative to the existing methods that can make the fracture investigation easier or more accurate. Generally, a suitable test sample and method should have simple geometry, simple testing process with conventional apparatus and fixtures, and should easily introduce different fracture modes including pure in-plane modes and mixed mode tensile-shear cases. In this study, a doughnut-shaped specimen (containing two-same line edge cracks and subjected to either diametral point load tension or compression), is designed and analyzed numerically for investigating mixed mode I/II fracture behavior. In this regard, by performing a large number of finite element analyses, the ability of such testing samples for introducing full ranges of pure mode I to pure mode II is demonstrated. Fracture parameters including mode I and mode II stress intensity factors are determined for the suggested specimen and for different geometrical and loading conditions (i.e., various kinds of specimens, configurations, crack lengths and different crack angles).

In the next sections, following description and introduction of the doughnut-shaped test sample, the process of determining the fracture parameters through numerical analyses are explained. Corresponding values of stress intensity factors are presented for different geometry and loading conditions of the doughnut-shaped test sample and the trends of these parameters for different input and affecting variables are obtained and discussed.

2. Doughnut-shaped specimen (DSS) under diametral point force

Fig. 4 shows the geometry and loading condition of the doughnut-shaped specimen (DSS) with center crack that was utilized for fracture investigations in this research. The DSS sample is a hollow disc or ring specimen with two equal length cracks of length a introduced at the inner circle of the ring with radii of R_i and R_o . The specimen can be subjected to either

diametral pin loading tension or compression as shown in Fig. 4a and Fig. 4b, respectively. The ring shape configuration with edge internal crack makes this sample a favorite geometry for conducting fracture toughness experiments on different engineering materials as stated in different works (Karimi et al., 2021; Dehghany et al., 2017). Altering the crack inclination angle (α) relative to the loading direction can result in changing the share of opening mode and sliding (shearing) mode in front of the crack tip. Hence, each angle will correspond to a specific in-plane mixed mode case (i.e., mode I/II mixity). In addition, the crack length and the inner and outer radii of the ring can affect the state of crack tip deformations and state of stress in the DSS sample either subjected to diametral tension or compression.

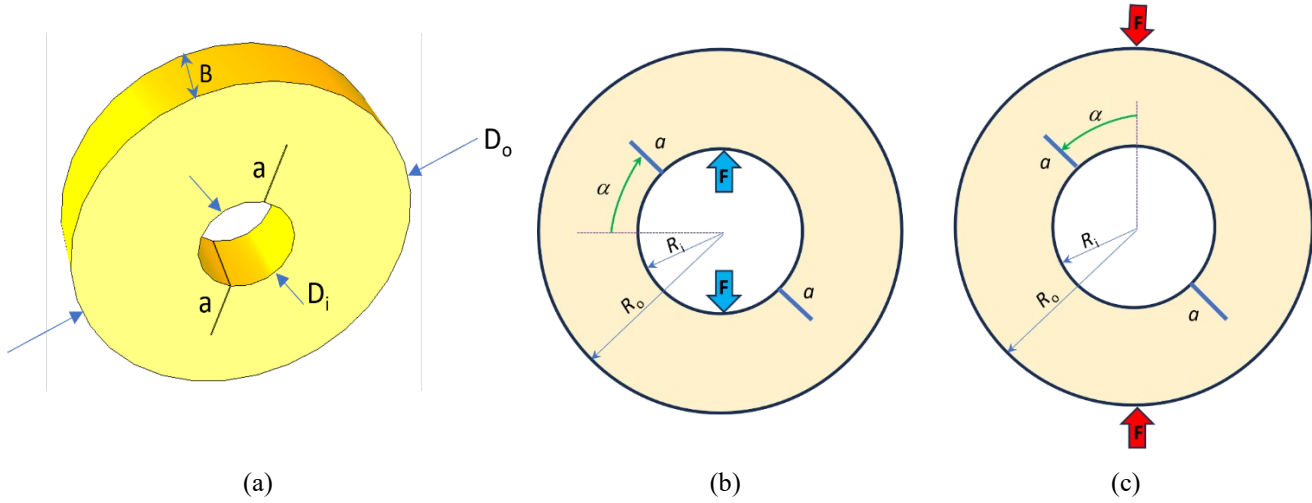


Fig. 4. (a) Geometry of doughnut-shaped specimen (DSS) subjected to (b) diametral point load tensile force (pin-loading tension) and (c) diametral point force compression.

The linear elastic stress field in the vicinity of a crack subjected to arbitrary far field loading is determined from the Williams infinite series expansion as below equation:

$$\sigma_{ij} = \frac{A}{\sqrt{2\pi r}} f(\theta) + H.O.T \quad (1)$$

where, r, θ are the components of polar system. The first term in this equation is singular term that is related to the stress intensity factors (SIFs). The other terms are related to higher order terms (H.O.T) that are non-singular and negligible compared to the singular terms. Accordingly, the stress components in polar system can be explained as following relations:

$$\sigma_{rr} = \frac{1}{\sqrt{2\pi r}} \cos \frac{\theta}{2} \left[K_I \left(1 + \sin^2 \frac{\theta}{2} \right) + K_{II} \left(\frac{3}{2} \sin \theta - 2 \tan \frac{\theta}{2} \right) \right] + H.O.T \quad (2)$$

$$\sigma_{r\theta} = \frac{1}{\sqrt{2\pi r}} \cos \frac{\theta}{2} \left[K_I \sin \theta \cos \frac{\theta}{2} + K_{II} (3 \cos \theta - 1) \right] + H.O.T \quad (3)$$

$$\sigma_{\theta\theta} = \frac{1}{\sqrt{2\pi r}} \cos \frac{\theta}{2} \left[K_I \cos^2 \frac{\theta}{2} - \frac{3}{2} K_{II} \sin \theta \right] + H.O.T \quad (4)$$

in which K_I and K_{II} are the modes I and II SIFs. In order to study the fracture behavior in any cracked sample and determine the onset of failure or fracture initiation direction or fracture path, first it is necessary to calculate the corresponding values of SIFs for any desired geometry, loading condition and mode mixity. The stress intensity factors (that describe the severity of stresses at crack tip) for the DSS specimen are written as below equations:

$$K_I = \frac{F\sqrt{\pi a}}{(R_o - R_i)B} \times Y_I \left(\bar{a}, \frac{R_i}{R_o}, \alpha \right) \quad (5)$$

$$K_{II} = \frac{F\sqrt{\pi a}}{(R_o - R_i)B} \times Y_{II} \left(\bar{a}, \frac{R_i}{R_o}, \alpha \right) \quad (6)$$

where Y_I and Y_{II} (geometry factors) are the normalized or non-dimensional form of K_I and K_{II} , respectively and $\bar{a} = a/(R_o - R_i)$. Based on Eq. (5) and Eq. (6) the SIF values are functions of applied load, crack length, dimensions of ring (its radii, R_o , R_i and thickness B) and crack inclination angle, α . The geometry factors (Y_I and Y_{II}) are also functions of \bar{a} , $\frac{R_i}{R_o}$ and α in the DSS specimen.

In the next section, these three fracture parameters are determined numerically for the doughnut-shaped specimen (DSS) under diametral compression and diametral tension loads.

3. Finite Element Analysis of DSS specimen

Finite element analysis combined with the concepts of linear elastic fracture mechanics provides a practical and convenient means to study the fracture characteristics of materials. Normal stresses create mode I or opening mode while mode II or shearing mode is caused by shear stresses. J-integral is widely used fracture mechanics concepts for determining the crack tip parameters under in-plane mode I-II fracture problems. In this study, the J-integral formulation was employed for analyzing the DSS specimen, as it is useful for a coarse mesh finite element analysis. Fig. 5 shows the mesh pattern of a full model Doughnut-Shaped Specimens (DSS), generated using ABAQUS finite element code. As a result, the entire specimen with constant thickness of 20 mm, fixed outer radius of ring ($R_o = 35$ mm) and variable crack lengths and inner radius of the ring was modeled using eight nodes collapsed quadrilateral elements and the mesh was refined around crack tip. It has been found that the calculated stress intensity factors and associated strain energy release rates used here did not vary when the number of the elements was doubled. Values for stress intensity factors were evaluated employing an interaction J-integral technique. The mechanical properties of a typical brittle material ($E = 6$ GPa and $\nu = 0.3$) were applied to the models of DSS samples. A reference load of $F = 1000$ N was also applied to the inner surface of the DSS sample in diametral tension manner and to the outer surface of the ring in diametral compression manner. Approximately 6500 eight-nodded quadratic elements were used for modeling the DSS specimen in ABAQUS code. A linear elastic finite element analysis was performed under a plane strain condition using root square $1/\sqrt{r}$ stress field singularity (suitable for linear elasticity).

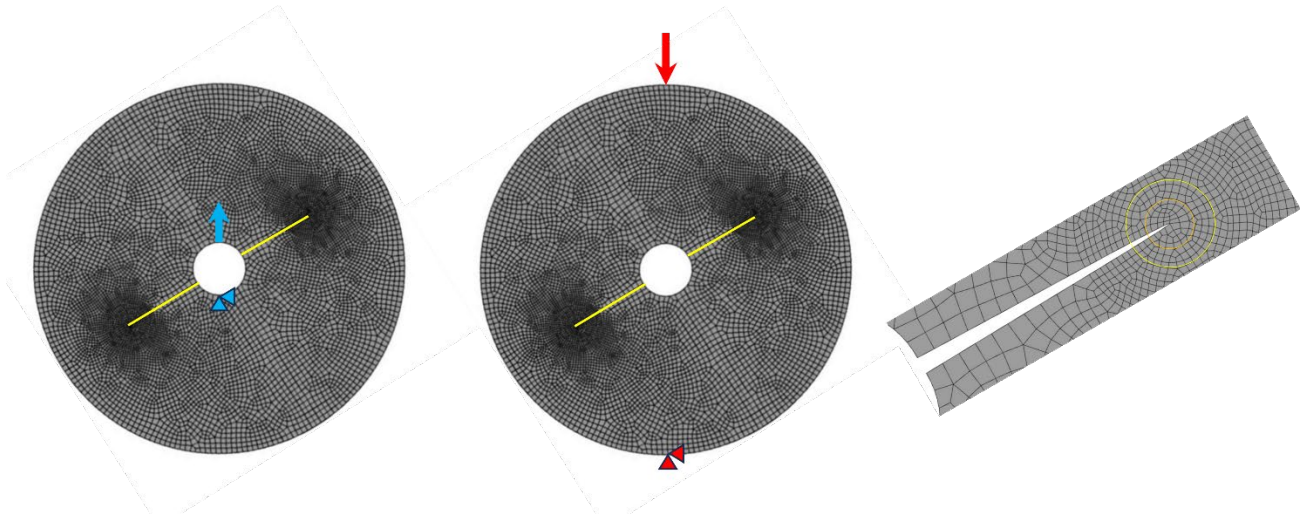


Fig. 5. Finite element mesh pattern of the entire and around the crack tip of the DSS specimen subjected to diametral compression and tension loads and crack tip elements.

4. Results and Discussion

In order to use DSS samples in practical fracture toughness determinations for any desired material, it is necessary to know first the corresponding values of mode I and mode II stress intensity factors. As the main aim of the current paper, the values of Y_I and Y_{II} (that are the geometry factors) are determined for a wide range and comprehensive geometry and loading conditions of the ring (DSS) sample. By knowing these geometry factors, the corresponding value of fracture toughness for any desired combinations of modes I and II can be determined experimentally by inserting the critical peak loads of tested material into Eq. (5) and Eq. (6).

Fig. 6 presents the variations of mode I geometry factor (Y_I) and mode II geometry factor (Y_{II}) for different crack lengths, inner ring radii and crack inclination angles (α) in the analyzed DSS samples subjected to diametral compression load. It is seen that the magnitude of Y_I depends on all investigated input variables (i.e., \bar{a} , $\frac{R_i}{R_o}$ and α). Generally, by increasing the crack inclination angle, the magnitude of Y_I reduces because of addition of shear mode deformation effects on the crack tip stress state. This reduction continues until an especial condition in which the corresponding value of Y_I (mode I geometry factor) reaches to zero value. The related crack inclination angle of this condition corresponds to mode II condition that is called α_{II} . The value of α_{II} depends on the type of applied loading (i.e., diametral compression or diametral tension). In contrary, mode II geometry factor increases by increasing the crack angle (α) for all crack lengths and ring geometries. Also, for any fixed crack angle, the corresponding value of Y_{II} becomes more by increasing \bar{a} value. According to the obtained results of Fig. 6, it can be concluded that the compressed DSS specimen can produce full combinations of opening-shearing mode deformations from pure mode I to pure mode II. While for the compressed DSS sample, pure mode I is obtained at $\alpha = 0^\circ$ for any crack length and ring geometry, α_{II} is achieved at the ranges of 20 to 35 degrees (from Fig. 6), depending on the crack length ratio and inner to outer radius of the ring sample. The corresponding value of α_{II} increases by increasing $\frac{R_i}{R_o}$ ratio and decreasing \bar{a} value. After such crack inclination angle, the DSS sample experience negative K_I that means the crack flanks are

compressed together. In addition, increasing the crack length ratio will result in increasing the corresponding value of Y_I mainly due to higher opening of larger crack length.

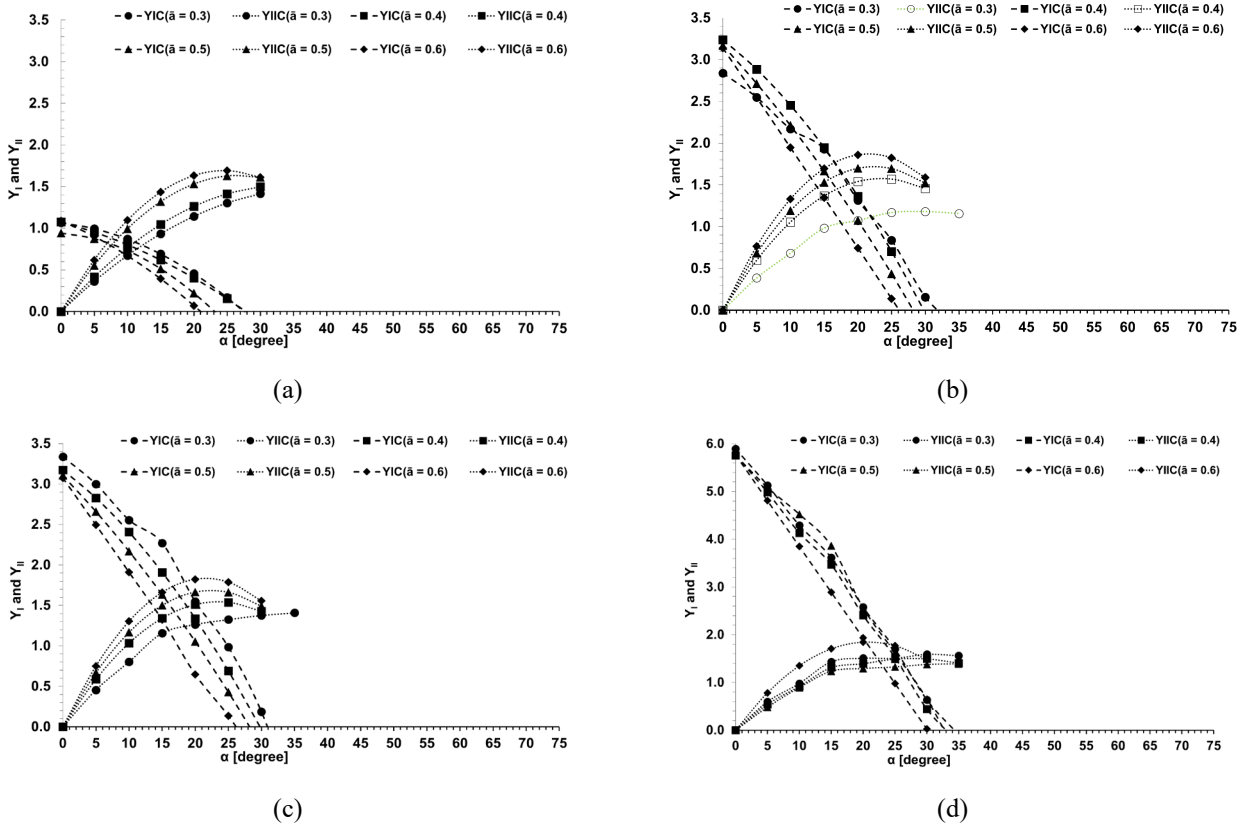


Fig. 6. Variations of mode I and mode II geometry factors (Y_{IC} and Y_{IIC}) for the analyzed DSS sample subjected to diametral compression and for different crack inclination angles and crack length ratios, (a) $R_i/R_o = 0.14$, (b) $R_i/R_o = 0.28$, (c) $R_i/R_o = 0.42$, (d) $R_i/R_o = 0.56$

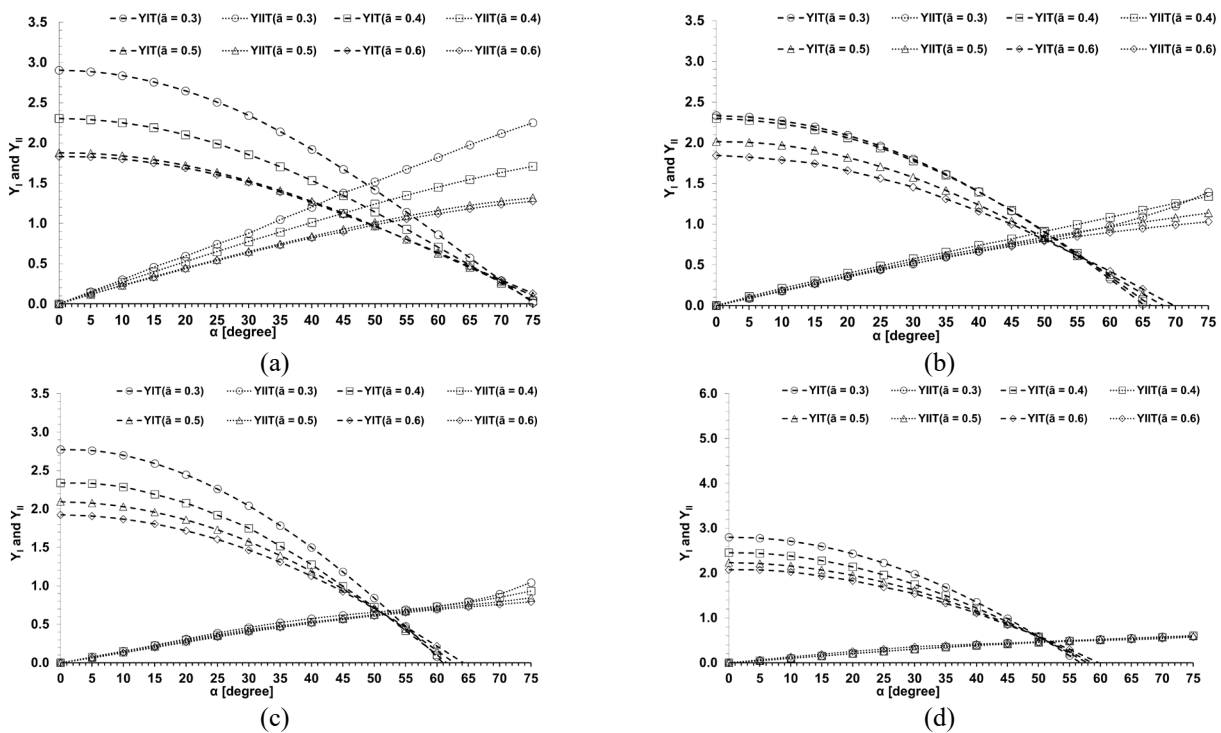


Fig. 7. Variations of mode I and mode II geometry factors (Y_{IT} and Y_{IIT}) for the analyzed DSS sample subjected to diametral tension and for different crack inclination angles and crack length ratios, (a) $R_i/R_o = 0.14$, (b) $R_i/R_o = 0.28$, (c) $R_i/R_o = 0.42$, (d) $R_i/R_o = 0.56$.

Similarly, **Fig. 7** presents the variations and trends of Y_I and Y_{II} parameters (Y_{IT} and Y_{IIT}) for the DSS specimen subjected to diametral tensile point loading and for different affecting parameters in this regard (i.e., crack length ratio, crack inclination angle and ring geometry). This figure reveals the similar trends of variations for the geometry factors of tensile loaded DSS samples observed earlier for the compressed DSS sample and discussed in **Fig. 6**. Indeed, the tensile DSS configuration can also provide all combinations of in-plane mode mixity ranging from tensile-shear to compressive shear crack deformations as well as pure modes I and II cases. Similar to compressed DSS samples, pure mode I condition is achieved at $a = 0^\circ$ for the tensile DSS sample for all geometry and loading conditions. but pure mode II condition is obtained for a DSS sample with inclined crack relative to the diametral tensile point loading direction. Based on **Fig. 7**, the range of a_{II} for the diametral tensile DSS sample varies from 57° to 75° and pure mode II crack inclination angle increases by R_i/R_o ratio and decreases the crack length ratio (i.e. \bar{a} parameter).

In order to better understand the role and influence of applied loading type (i.e., diametral compression and diametral tension point loading) on the geometry factors of the DSS sample, **Fig. 8** compares the Y_I and Y_{II} curves of both DSS type configurations for different ring geometries and crack inclination angles. These curves reveal that type of loading has a significant impact on the stress intensity factors or geometry factors. For example, the corresponding value of mode I stress intensity factor (or Y_I) for the diametral tensile DSS sample is higher than the Y_I value of the compressed DSS sample. In contrast, for any given crack angle (up to $a = 35^\circ$), the corresponding value of Y_{II} in the compressed DSS specimen is higher than the tensile DSS configuration. In addition, the tensile DSS sample shows less sensitivity to the crack angle compared to the compressed DSS configuration, because there is a large interval between pure mode I and mode II (typically about 60 degrees) compared to the compressed DSS configuration in which only about 25-degrees interval exists between pure mode I and pure mode II cases. Hence, any error in price setting of the crack direction relative to the loading orientation in the compressed DSS sample will result in higher discrepancy in the determined fracture toughness values under mixed mode I/II loading case.

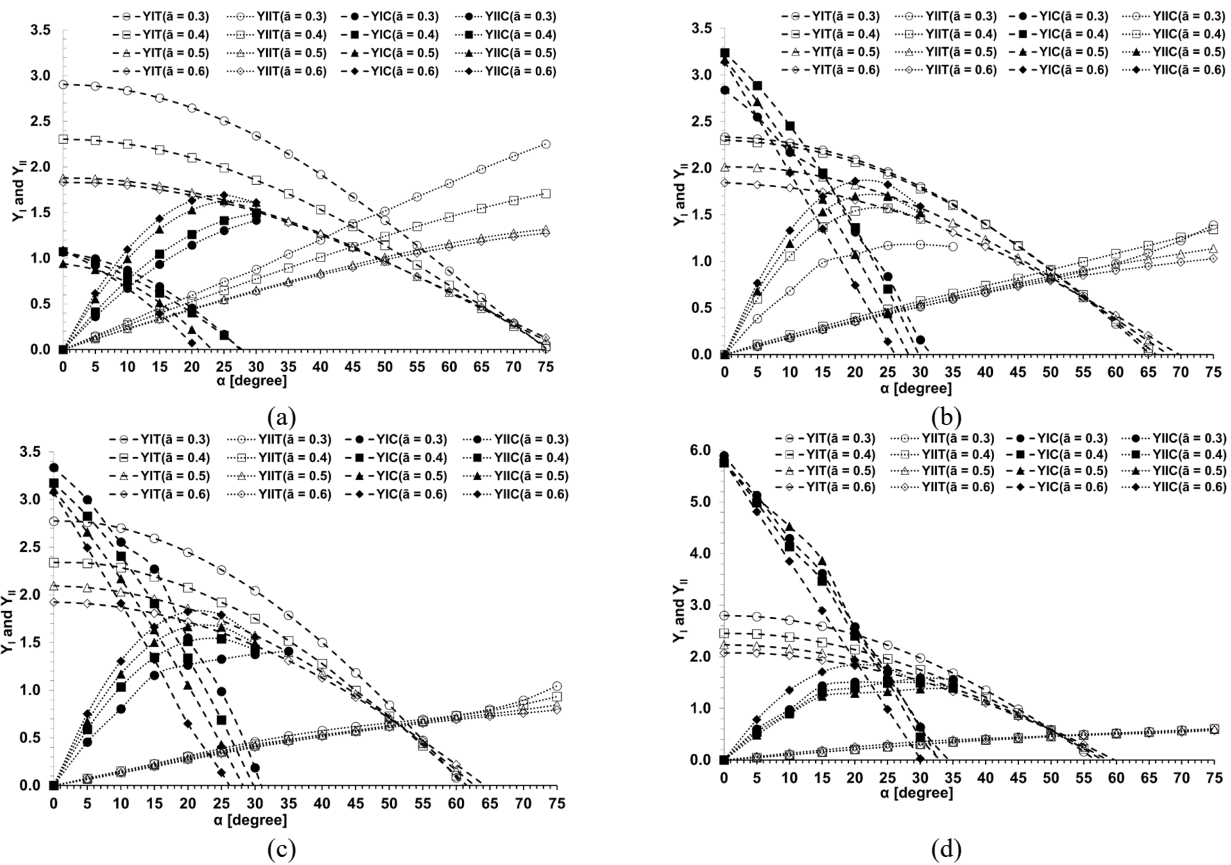


Fig. 8. Comparison of mode I and mode II geometry factors (Y_I and Y_{II}) for the analyzed DSS sample subjected to both diametral compression and diametral tension point loads for different crack inclination angles and crack length ratios, (a) $R_i/R_o = 0.14$, (b) $R_i/R_o = 0.28$, (c) $R_i/R_o = 0.42$, (d) $R_i/R_o = 0.56$

5. Conclusions

Two hollow disc (ring) shape configurations containing internal edge crack and subjected to diametral compression point load (compressed DSS) and diametral pin loading point force (tensile DSS) were analyzed in this research. Mode I and mode II stress intensity factors (SIFs) and their normalized forms (called geometry factors, Y_I and Y_{II}) were determined through extensive finite element simulations of the DSS sample in ABAQUS software. The following concluding remarks can be outlined:

- Both tensile and compressed DSS samples were able to introduce full ranges of mode I and mode II mixities including pure mode I, pure mode II, mixed mode tensile-shear and mixed mode compression shear by altering the geometrical and loading factors and in particular the crack inclination angle.
- type of loading (i.e. diametral compression or diametral tension) was noticeable in the magnitude and variations of modes I and II SIFs. For example, in the pure mode I case, the corresponding value of mode I geometry factor (Y_I) obtained from the compressed DSS sample was noticeably greater than the value of Y_I obtained from the tensile DSS.
- Pure mode II crack inclination angle (α_{II}) for the compressed DSS sample were obtained at angles ranging from 20 to 35° depending on the crack length ratio and inner diameter of the ring. This range for the tensile DSS sample was varied in the range of 55 to 75 degrees. Hence, the crack tip parameters in the compressed DSS sample are more sensitive to the crack inclination angle compared to the tensile DSS sample.
- Both geometry factors increased by reducing the crack length ratio and increasing the inner to outer radius ratio of the ring.

Acknowledgments

Mohammad Reza Mohammad Aliha acknowledges the TÜBİTAK (Grant No. 2221-1059B212200747) program for visiting scientists on sabbatical leave to visit Gebze Technical University, Turkey.

References

- Aliha, M. R. M., Ayatollahi, M. R., Smith, D. J., & Pavier, M. J. (2010). Geometry and size effects on fracture trajectory in a limestone rock under mixed mode loading. *Engineering Fracture Mechanics*, 77(11), 2200–2212.
- Aliha, M. R. M., Bahmani, A., & Akhondi, S. (2016). Mixed mode fracture toughness testing of PMMA with different three-point bend type specimens. **European Journal of Mechanics - A/Solids*, 58*, 148–162.
- Aliha, M. R. M., Ghoreishi, S. M. N., Imani, D. M., Fotoohi, Y., & Berto, F. (2020). Mechanical and fracture properties of aluminium cylinders manufactured by orbital friction stir welding. *Fatigue & Fracture of Engineering Materials & Structures*, 43(7), 1514–1528.
- Aliha, M. R. M., Hosseinpour, G. R., & Ayatollahi, M. R. (2013). Application of cracked triangular specimen subjected to three-point bending for investigating fracture behavior of rock materials. *Rock Mechanics and Rock Engineering*, 46(5), 1023–1034.
- Aliha, M. R. M., Mahdavi, E., & Ayatollahi, M. R. (2017). The influence of specimen type on tensile fracture toughness of rock materials. *Pure and Applied Geophysics*, 174, 237–1253.
- Aliha, M. R. M., reza Karimi, H., & Abedi, M. (2022). The role of mix design and short glass fiber content on mode-I cracking characteristics of polymer concrete. *Construction and Building Materials*, 317, Article 126139.
- Ameri, B., Taheri-Behrooz, F., & Aliha, M. R. M. (2021). Evaluation of the geometrical discontinuity effect on mixed-mode I/II fracture load of FDM 3D-printed parts. *Theoretical and Applied Fracture Mechanics*, 113, Article 102953.
- Bahmani, A., Aliha, M. R. M., Sarbijan, M. J., & Mousavi, S. S. (2020). An extended edge-notched disc bend (ENDB) specimen for mixed-mode I+II fracture assessments. *International Journal of Solids and Structures*, 193, 239–250.
- Bahmani, A., Farahmand, F., Janbaz, M. R., Darbandi, A. H., Ghesmati-Kucheki, H., & Aliha, M. R. M. (2021). On the comparison of two mixed-mode I+III fracture test specimens. *Engineering Fracture Mechanics*, 241, Article 107434.
- Bahmani, A., & Nemati, S. (2021). Fracture resistance of railway ballast rock under tensile and tear loads. *Engineering Solid Mechanics*, 9(3), 271–280.
- Baradaran, S., Aliha, M. R. M., Maleki, A., & Underwood, B. S. (2024). Fracture properties of asphalt mixtures containing high content of reclaimed asphalt pavement (RAP) and eco-friendly PET additive at low temperature. *Construction and Building Materials*, 449, Article 138426.
- Benderly, D., Rezek, Y., Zafran, J., & Gorni, D. (2004). Effect of composition on the fracture toughness and flexural strength of syntactic foams. *Polymer Composites*, 25(2), 229–236.
- Bidadi, J., Akbardoost, J., & Aliha, M. R. M. (2020). Thickness effect on the mode III fracture resistance and fracture path of rock using ENDB specimens. *Fatigue & Fracture of Engineering Materials & Structures*, 43(2), 277–291.
- Chen, C. H., Chen, C. S., & Wu, J. H. (2008). Fracture toughness analysis on cracked ring disks of anisotropic rock. *Rock Mechanics and Rock Engineering*, 41, 539–562.
- Choupani, N. (2008). Experimental and numerical investigation of the mixed-mode delamination in Arcan laminated specimens. *Materials Science and Engineering: A*, 478(1–2), 229–242.
- Choupani, N., & Torun, A. (2022). Fracture characterization of bonded composites: A comparative study. *Engineering Solid Mechanics*, 10(1), 109–116.
- Dehghany, M., Saeidi Googarchin, H., & Aliha, M. R. M. (2017). The role of first non-singular stress terms in mixed mode brittle fracture of V-notched components: An experimental study. *Fatigue & Fracture of Engineering Materials & Structures*, 40(4), 623–641.
- Dharmawan, F. S. G. H., Simpson, G., Herszberg, I., & John, S. (2006). Mixed mode fracture toughness of GFRP composites. *Composite Structures*, 75(1–4), 328–338.

- Erarslan, N., & Aliha, M. R. M. (2025). Fracture and damage analysis of cement-stabilized fine and coarse grain soils under static and cyclic loading using chevron-notched SCB specimen. *Fatigue & Fracture of Engineering Materials & Structures*, 48(6), 2708–2724.
- Fakhri, M., Amoosoltani, E., & Aliha, M. R. M. (2017). Crack behavior analysis of roller compacted concrete mixtures containing reclaimed asphalt pavement and crumb rubber. *Engineering Fracture Mechanics*, 180, 43–59.
- Fakhri, M., Yousefian, F., Amoosoltani, E., Aliha, M. R. M., & Berto, F. (2021). Combined effects of recycled crumb rubber and silica fume on mechanical properties and mode I fracture toughness of self-compacting concrete. *Fatigue & Fracture of Engineering Materials & Structures*, 44(10), 2659–2673.
- Fuan, S., Ke, M., Kanghe, L., Kun, L., & Aliha, M. R. M. (2021). Influence of specimen geometry on mode I fracture toughness of asphalt concrete. *Construction and Building Materials*, 276, Article 122181.
- Gliszczynski, A., & Wiącek, N. (2021). Experimental and numerical benchmark study of mode II interlaminar fracture toughness of unidirectional GFRP laminates under shear loading using the end-notched flexure (ENF) test. *Composite Structures*, 258, Article 113190.
- Gu, X., Cheng, T., Zhang, F., & Aliha, M. R. M. (2023). Experimental and theoretical framework for illustrating the dependency of fracture toughness with tensile, bending, and compression loading in asphaltic samples. *Fatigue & Fracture of Engineering Materials & Structures*, 46(9), 3321–3341.
- Haddadi, E., Choupani, N., & Abbasi, F. (2016). Experimental investigation on the mixed-mode fracture of rubber-toughened PMMA using essential work of fracture method. *Engineering Fracture Mechanics*, 162, 112–120.
- Hanson, J. A., Hardin, B. O., & Mahboub, K. (1994). Fracture toughness of compacted cohesive soils using ring test. *Journal of Geotechnical Engineering*, 120(5), 872–891.
- He, J., Liu, L., Yang, W., & Aliha, M. R. M. (2022). Influence of testing method on mode II fracture toughness (KIIC) of hot mix asphalt mixtures. *Fatigue & Fracture of Engineering Materials & Structures*, 45(10), 2940–2957.
- Heydari, M. H., Choupani, N., & Shamel, M. (2011). Experimental and numerical investigation of mixed-mode interlaminar fracture of carbon-polyester laminated woven composite by using arcane set-up. *Applied Composite Materials*, 18, 499–511.
- Imani, D. M., Aliha, M. R. M., Linul, E., & Marsavina, L. (2022). A suitable mixed mode I/II test specimen for fracture toughness study of polyurethane foam with different cell densities. *Theoretical and Applied Fracture Mechanics*, 117, Article 103171.
- Jia, R., Zhao, L., Curti, R., & Gong, X. (2021). Determination of pure mode-I fracture toughness of multidirectional composite DCB specimens. *Engineering Fracture Mechanics*, 252, Article 107776.
- Karimi, H. R., Aliha, M. R. M., Mousavi, A., Ghoreishi, S. M. N., & Sadowski, T. (2025). Shear strength and shear energy measurement of brittle materials using two novel disc and beam shape configurations under asymmetrical three-point bend loading. *Construction and Building Materials*, 493, Article 143165.
- Karimi, H. R., Khedri, E., Aliha, M. R. M., & Mousavi, A. (2022). A comprehensive study on ring shape specimens under compressive and tensile loadings for covering the full range of I+II fracture modes of gypsum material. *International Journal of Rock Mechanics and Mining Sciences*, 160, Article 105265.
- Marşavina, L., & Linul, E. (2020). Fracture toughness of rigid polymeric foams: A review. *Fatigue & Fracture of Engineering Materials & Structures*, 43(11), 2483–2514.
- Marsavina, L., Constantinescu, D. M., Linul, E., Voiconi, T., & Apostol, D. A. (2015). Shear and mode II fracture of PUR foams. *Engineering Failure Analysis*, 58, 465–476.
- Mohammad Aliha, M. R., Ghesmati Kucheki, H., & Asadi, M. M. (2021). On the use of different diametral compression cracked disc shape specimens for introducing mode III deformation. *Fatigue & Fracture of Engineering Materials & Structures*, 44(11), 3135–3151.
- Mousavi, A., Aliha, M. R. M., & Imani, D. M. (2020). Effects of biocompatible Nanofillers on mixed-mode I and II fracture toughness of PMMA base dentures. *Journal of the Mechanical Behavior of Biomedical Materials*, 103, Article 103566.
- Mousavi, A., Aliha, M. R. M., Khoramishad, H., Karimi, H. R., Choupani, N., & Sadowski, T. (2025a). Opening-tearing mixed-mode fracture behavior of rock using ENDB, ENDC, DNDC, SCB, TPB-IC, SENB, and ATPB specimens. *Engineering Solid Mechanics*, 13(1), 1–14.
- Mousavi, A., Aliha, M. R. M., Khoramishad, H., & Karimi, H. R. (2025b). The effect of non-singular term (T-stress) on mode I/III cracking parameters of brittle materials, Numerical and experimental study using different beam and disc shape specimens made of marble rock. *Forces in Mechanics*, 18, Article 100303.
- Najjar, S., Moghaddam, A. M., Sahaf, A., & Aliha, M. R. M. (2022). Experimental and statistical exploring for mixed-mode (I&II) fracture behavior of cement emulsified asphalt mortar under freeze–thaw cycles and aging condition. *Theoretical and Applied Fracture Mechanics*, 122, Article 103643.
- Noury, P. M., Sheno, R. A., & Sinclair, I. (1998). On mixed-mode fracture of PVC foam. *International Journal of Fracture*, 92(2), 131–151.
- Pereira, F. A. M., de Moura, M. F. S. F., Dourado, N., Morais, J. J. L., Xavier, J., & Dias, M. I. R. (2018). Determination of mode II cohesive law of bovine cortical bone using direct and inverse methods. *International Journal of Mechanical Sciences*, 138, 448–456.
- Pierron, F., & Vautrin, A. (1998). Measurement of the in-plane shear strengths of unidirectional composites with the Iosipescu test. *Composites Science and Technology*, 57(12), 1653–1660.

- Pugna, A., Negrea, R., Linul, E., & Marsavina, L. (2020). Is fracture toughness of PUR foams a material property? A statistical approach. *Materials*, *13*(21), Article 4868.
- Razavi, N., & Berto, F. (2019). A new fixture for fracture tests under mixed mode I/II/III loading. *Fatigue & Fracture of Engineering Materials & Structures*, *42*(9), 1874–1888.
- Saenz, E. E., Carlsson, L. A., & Karlsson, A. (2011). Characterization of fracture toughness (G_c) of PVC and PES foams. *Journal of Materials Science*, *46*, 3207–3215.
- Saesaei, A. H., Sahaf, A., Najjar, S., & Aliha, M. R. M. (2024). Laboratory investigation on the fracture toughness (Mode I) and durability properties of eco-friendly cement emulsified asphalt mortar (CRTS II) exposed to acid attack. *Case Studies in Construction Materials*, *20*, Article e02719.
- Santos, M. A. S., & Campilho, R. D. S. G. (2017). Mixed-mode fracture analysis of composite bonded joints considering adhesives of different ductility. *International Journal of Fracture*, *207*(1), 55–71.
- Shahbazian, B., Mirsayar, M. M., Aliha, M. R. M., Darvish, M. G., Asadi, M. M., & Haghighatpour, P. J. (2022). Experimental and theoretical investigation of mixed-mode I/II and I/III fracture behavior of PUR foams using a novel strain-based criterion. *International Journal of Solids and Structures*, *258*, Article 111996.
- Shameli, M., & Choupani, N. (2016). Fracture criterion of woven glass-epoxy composite using a new modified mixed-mode loading fixture. *International Journal of Applied Mechanics*, *8*(2), Article 1650015.
- Szekrényes, A. (2009). Improved analysis of the modified split-cantilever beam for mode-III fracture. *International Journal of Mechanical Sciences*, *51*(9–10), 682–693.
- Tutluoglu, L., Batan, C. K., & Aliha, M. R. M. (2022). Tensile mode fracture toughness experiments on andesite rock using disc and semi-disc bend geometries with varying loading spans. *Theoretical and Applied Fracture Mechanics*, *119*, Article 103325.
- Vantadori, S., Carpinteri, A., Cerioni, R., Ronchei, C., Scorza, D., Zanichelli, A., & Marsavina, L. (2023). Fracture toughness of a rigid polyurethane foam: Experimental and numerical investigation by varying the specimen sizes. *Fatigue & Fracture of Engineering Materials & Structures*, *46*(10), 3654–3666.
- Wu, J., Wang, H., Mao, L., & Aliha, M. R. M. (2023). Composition optimization of PMMA base denture reinforced with different percentages of Nano Hydroxyapatite and alumina particles to obtain highest K_{Ic} and K_{IIc} values using hybrid IWO/PSO algorithm. *Theoretical and Applied Fracture Mechanics*, Article 104090.
- Zhang, T., Wang, S., & Wang, W. (2019). A unified energy release rate based model to determine the fracture toughness of ductile metals from unnotched specimens. *International Journal of Mechanical Sciences*, *150*, 35–50.



© 2026 by the authors; licensee Growing Science, Canada. This is an open access article distributed under the terms and conditions of the Creative Commons Attribution (CC-BY) license (<http://creativecommons.org/licenses/by/4.0/>).